Journal of Exploratory Research in Pharmacology **2021** vol. 7(1) | 17–29
DOI: 10.14218/JERP.2021.00050

Original Article

Potential SARS-CoV-2 Spike Protein–ACE2 Interface Inhibitors: Repurposing FDA-approved Drugs

Valentina L. Kouznetsova[1,2#], Aidan Zhang[3#], Mark A. Miller[1#], Mahidhar Tatineni[1], Jerry P. Greenberg[1] and Igor F. Tsigelny[1,2,4*]

[1]*San Diego Supercomputer Center, University of California, San Diego, California, USA;* [2]*BiAna, California, USA;* [3]*REHS program, San Diego Supercomputer Center, University of California, San Diego, California, USA;* [4]*Department of Neurosciences, University of California, San Diego, California, USA*

Received: November 08, 2021 | **Revised:** November 23, 2021 | **Accepted:** December 10, 2021 | **Published:** December 24, 2021

Abstract

Background and objectives: The SARS-CoV-2 virus Spike (S) protein binds to an angiotensin-converting-enzyme 2 receptor (ACE2) on the surface of cells to allow viral DNA entry. Given the plenitude of FDA-approved antiviral drugs, we aimed to screen those that may be repurposed for treating SARS-CoV-2 infections.

Methods: Using the crystal structure of SARS-CoV-2 Spike complexed with ACE2 (PDB ID: 6VW1) as a template, we developed a pharmacophore model of functional centers of the SARS-CoV-2 Spike protein inhibitor-binding domain. The conformations of these compounds underwent 3D fingerprint similarity clusterization, followed by docking of possible conformers to the binding site of ACE2. A similar protocol was followed for a set of randomly-selected compounds. Molecular dynamics was perform to confirm the stability of the selected drugs bound to ACE2.

Results: Based on the model, we conducted a pharmacophore search from a conformational database of FDA-approved drugs. From the 379 compounds identified as potential inhibitors of SARS-CoV-2, 152 compounds with the best scores were selected based on maximal hydrogen-bond and hydrophobic interactions. The average free energies of the docking interaction for the selected compounds were better than those of random compounds. The obtained drug list includes inhibitors of HIV, HCV, CMV, ZIKV, HMPV, and RVFV as well as a set of drugs that have demonstrated some activity in MERS, SARS-CoV, and SARS-CoV-2 therapy.

Conclusions: Using a set of computational methods, we predicted the FDA-approved drugs that might bind to the interface of ACE2 protein and Spike protein of SARS-CoV-2 and prevent binding between Spike and ACE2. In further works, we recommend testing the selected compounds for treatment of COVID-19.

Keywords: COVID-19; SARS-CoV-2; Pharmacophore; Docking; Molecular dynamics; Repurposing.

Abbreviations: 3D, three-dimensional; ACE2, angiotensin-converting enzyme 2; CMV, cytomegalovirus; CoV, coronavirus; COVID-19, coronavirus disease 2019; DB, database; DFE, docking free energy; DMPC, dimyristoylphosphatidylcholine; FAD, flavin adenine dinucleotide; GpiDAPH3, Graph three-point pharmacophore (fingerprint); HCV, hepatitis C virus; HIV, human immunodeficiency virus; HMPV, human metapneumovirus; IO, input/output (file system); MD, molecular dynamics; MERS, Middle East respiratory syndrome; MOE, Molecular Operating Environment; NAMD, Nanoscale Molecular Dynamics; RBD, receptor-binding domain; RVFV, Rift Valley fever virus; S, Spike (protein); S1, Spike protein 1; S2, Spike protein 2; SARS, severe acute respiratory syndrome; SDSC, San Diego Supercomputer Center; SSD, solid-state drive; VMD, Visual Molecular Dynamics; ZIKV, Zika virus; ZINC, "ZINC is not commercial" (database).

***Correspondence to**: Igor F. Tsigelny, San Diego Supercomputer Center, University of California, San Diego, California 92093-0505, USA; Department of Neurosciences, University of California, San Diego, California 92093-0505, USA. ORCID: https://orcid.org/0000-0002-7155-8947. Tel: +1-858-457-0595, Email: itsigeln@ucsd.edu

[#]These authors contributed equally to this work.

How to cite this article: Kouznetsova VL, Zhang A, Miller MA, Tatineni M, Greenberg JP, Tsigelny IF. Potential SARS-CoV-2 Spike Protein–ACE2 Interface Inhibitors: Repurposing FDA-approved Drugs. *J Explor Res Pharmacol* 2021;7(1):17–29. doi: 10.14218/JERP.2021.00050.

Introduction

The ongoing COVID-19 pandemic has resulted over 225 million confirmed cases and claimed more than 4.62 million lives worldwide (as of September 14, 2021). The SARS-CoV-2 virus that causes COVID-19 is closely related to SARS-CoV, the coronavirus responsible for the severe acute respiratory syndrome (SARS)

outbreak in 2002. Although effective vaccines are now being implemented in healthcare practice, given the magnitude of the pandemic and the high death rate from infection, there is still a need to find effective treatment strategies for infected patients.

Coronavirus infection begins with binding of the viral Spike (S) protein to a cellular receptor, which is followed by conformational changes that lead to fusion of the virus with the cellular membrane.[1] The Spike protein of SARS-CoV-2 consists of subunits S1 and S2.[2] In the case of SARS-CoV-2 as well as SARS-CoV, the subunit S1 binds to the angiotensin-converting enzyme 2 (ACE2) receptor,[3–5] while the subunit S2 forms a six-helical bundle via the two-heptad repeat domain that supports cell membrane fusion.[2] The crystal structures of complexes between the viral S protein and ACE2 suggest that the two viruses have similar but not identical modes of binding,[4,6–8] which is consistent with the overall 76% identity between the SARS-CoV-2 S protein and SARS-CoV S protein (50% identity within the receptor-binding domain).[5] Binding of the protein subunit S1 to the ACE2 receptor is followed by priming of S protein by extracellular TMPRSS2, a serine protease.[9–11] Priming changes the conformation of S protein, allowing the viral particle to fuse with the cellular membrane and, subsequently, the nucleic acid payload to enter the host cell. Priming by extracellular proteases is required for infectivity, whereby inhibition of the proteases neutralizes the virus.[3]

Two basic strategies are available to prevent entry of viral DNA into the cell. The first strategy prevents binding of the S protein to the ACE2 protein using monoclonal antibodies directed at the S-protein receptor-binding domain (RBD) to inhibit attachment of the virus. The second strategy prevents binding to ACE2 using compounds that modify its glycan component[12] or compounds that interfere with or block the binding site of the RBD. The second strategy can be accomplished using compounds that inhibit other viral proteins or completely new compounds that fit the residue pattern of the ACE2–S1 interface.

Techniques to accomplish these two strategies have both advantages and disadvantages for patient treatment. For instance, the use of monoclonal antibodies depends on the availability of antibodies with a required specificity. While available monoclonal antibodies against SARS-CoV are not effective against SARS-CoV-2,[13,14] their neutralizing monoclonal antibodies derived from recovered patients[15,16] have been used successfully.[17] In addition, the use of monoclonal antibodies is now a widely-used treatment strategy for patients with mild symptoms. For patients with more severe symptoms, alternative strategies are still needed.

Targeting host enzyme activities, such as the catalytic site of ACE2 or extracellular proteases, are problematic, as these are likely to have undesirable and potentially deleterious side effects. On the other hand, affinity of the viral S protein for ACE2 seems to be unrelated to its enzymatic activity.[18] Crystal structures have shown that the RBD/ACE2 interface is distinct from the catalytic site,[4,6] suggesting that it can possibly interfere with the interaction between S and ACE2 without inhibiting the activity of ACE2. Herein, we report a virtual screen for compounds that will interfere with S protein binding to ACE2 at the S/ACE2 interaction site.

Methods

Pharmacophore design and use

By analyzing the binding interface of the Spike protein with ACE2, we elucidated several possible interactions between ACE2 and this protein (PDB ID: 6VW1),[19] providing a potential target for developing a pharmacophore model based on the pharmacophore centers corresponding to the S1 subunit interacting with ACE2 (Fig. 1). Using the Molecular Operating Environment (MOE) package (Chemical Computing Group ULC, Montreal, Quebec, Canada),[20] we constructed a pharmacophore model of the binding interface including 16 features: 4 donors, 5 acceptors, 2 donors or/and acceptors, and 5 hydrophobic features (Fig. 2). We conducted a pharmacophore search with the whole and partial pharmacophore models using an internally created conformational database of FDA-approved drugs, containing 2,356 drugs and 600,000 conformations. The search was performed allowing for partial matches: seven and six of sixteen features. The search of seven of sixteen features (Search 1) identified 127 compounds with 64,449 conformations while the search of six of sixteen features (Search 2) identified 379 compounds with 806,486 conformations. Because Search 1 is absorbed by Search 2, we selected 152 compounds from Search 2 based on the greatest number of hydrogen-bonds and hydrophobic interactions in the best docked orientation. Then, we clustered the selected 152 compounds using the Compute/Fingerprint/Clusters application of the MOE Database Viewer, which calculates fingerprints for each molecule and a similarity matrix with Tanimoto similarity metric. From the similarity matrix, comparing to similarity threshold *S*, similar fingerprints are determined from which, using Tanimoto coefficient again and overlap threshold *O*, clusters were selected. A fingerprint GpiDAPH3 and similarity–overlap parameter $SO = 45\%$ were used to elucidate the common structure-functional features of the groups of compounds to enhance further drug development based on similarity of the selected drugs.

Docking of drug conformers using the supercomputer Comet

To dock the selected compounds, we used the crystal structure of the complex containing SARS-CoV-2 Spike protein and ACE2 (PDB ID: 6VW1). A binding interface was defined based on 14 residues of the protein's S1 subunit with 29 contacts with ACE2. Figure 1 indicates that the S1–ACE2 interface could be divided into two interface sites: Site 1 includes ACE2 residues Gln24, Lys26, Thr27, Asp30, Lys31, His34, Glu35, Leu79, Met82, and Tyr83; and Site 2 contains residues Glu37, Asp38, Tyr41, Gln42, Gly352, Lys353, Gly354, Asp355, and Arg357.

To validate the specificity of the docked compounds, docking of random compounds was also conducted. A random number generator without repetition was used to obtain 100 random compounds and to select entries from the ZINC database that correspond to the random numbers obtained.

Conformers of each of the 152 selected compounds and 100 random compounds were generated using Compute/Conformations/Import application of MOE, which created 250 or more conformations per compound through a stochastic search. The application generated low-energy conformations of a collection of compounds and stored them in a molecular database, containing a total of 13,126 drug conformers from the selected compounds and 15,596 conformers from the randomly selected compounds.

OpenBabel [http://openbabel.org (accessed September 28, 2021)] was used to convert the pdb files into pdbqt format, which is necessary for using AutoDock Vina.[21] The pdbqt files were prepared for both ligands and proteins. The binding sites of ACE2 were defined as a box that encompasses residues of the binding site. The resulting log files include poses generated by the AutoDock Vina, scores as an affinity estimation, energies of compound–protein interaction, and RMSD as geometric criteria of similarity.

AutoDock Vina (version 1.1.2) was run on the Comet supercomputer at the San Diego Supercomputer Center (SDSC) to ex-

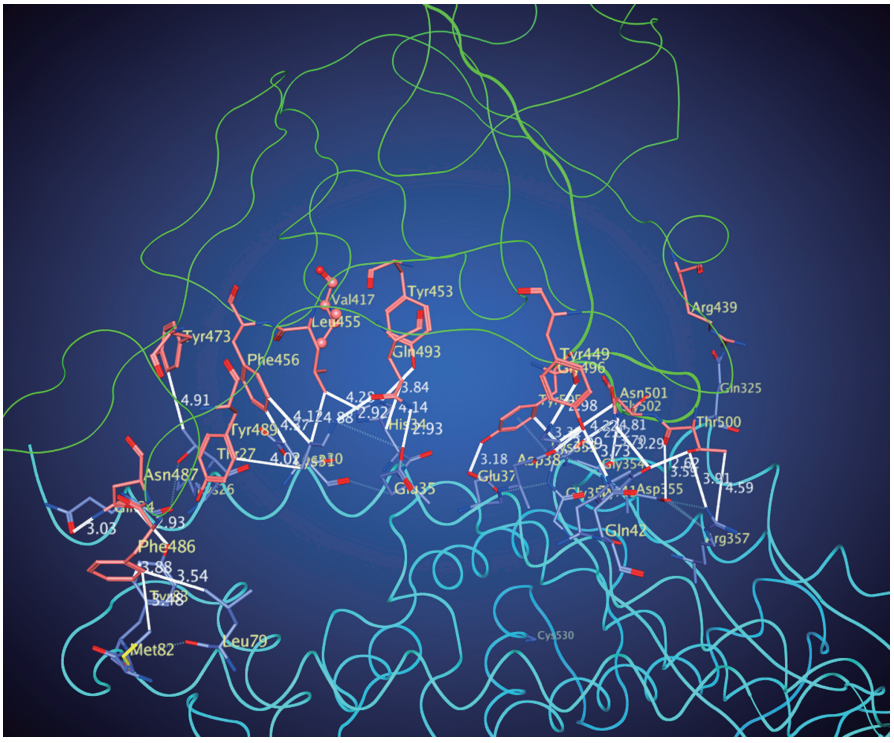

Fig. 1. Interface between S1 subunit of S protein (green ribbon, orange residues) and ACE2 (cyan ribbon, light-blue residues). One can see that the interface splits into Site 1 on the left and Site 2 on the right.

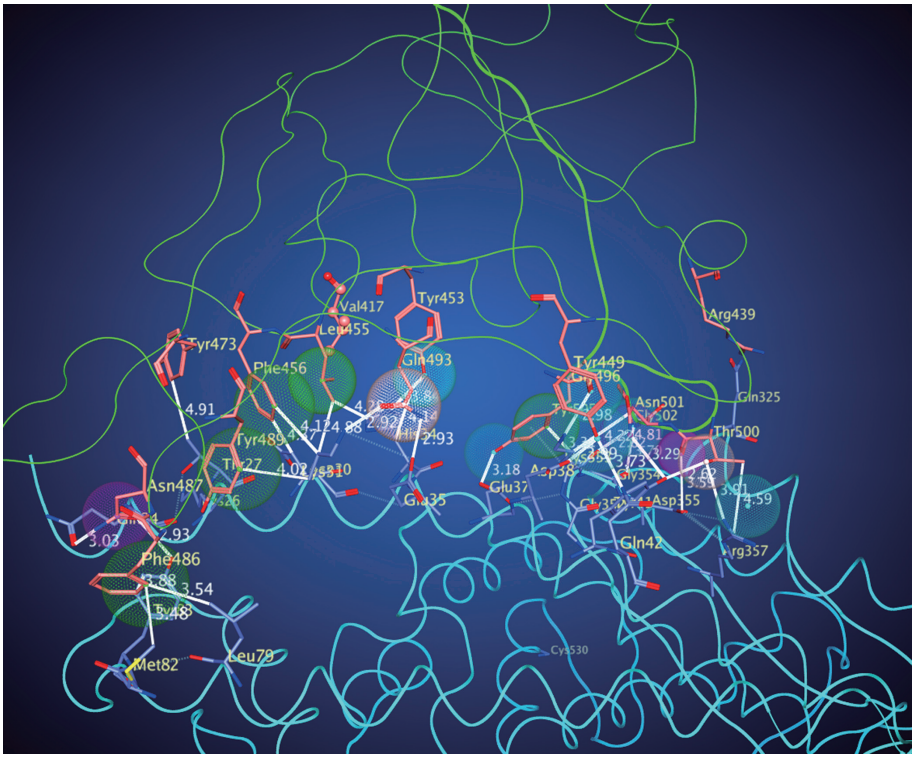

Fig. 2. S1 subunit of Spike protein (green ribbon, orange residues) binding domain and a pharmacophore constructed based on the S1 subunit. Pharmacophore center colors: cyan–acceptors, magenta–donors, green–hydrophobes, and pink–donors and/or acceptors. ACE2 receptor: cyan ribbon, light-blue residues. ACE2, angiotensin-converting enzyme 2.

plore docking of the 28,722 conformers (13,126 + 15,596), including both drugs and random compounds. This ultimately resulted in 258,498 total docking poses, as Autodock Vina outputs 9 poses per conformer. Details of the Comet computer used are presented in our previous publications.[22,23]

Final filtration of the binding poses was conducted based on the average distance of the docked compounds to the ACE2 binding residues. We calculated an upper boundary on the average distance between ligand atoms and binding residue side chain atoms. Binding poses with an average distance exceeding this upper boundary were filtered out, then poses with the lowest binding energies were selected from the remaining binding poses.

Docking workflow

Docking tasks were split up into a total of 34 separate jobs, most of which were run simultaneously (some cases were rerun with smaller splits to fit within wall clock limits on Comet) with 500–5,800 drug conformers docked in each job. The splits were made to keep the runtime between 24–48 h. During the simulations, the input dataset was extracted from aggregated zip files into local SSD space on the compute nodes. At the end of the simulation, the output files were aggregated into zip files and copied back to the home directory. This approach was successful in mitigating the IO loads on the main file system. All individual docking computations were conducted using eight cores (the parallelism is limited by the exhaustiveness parameter, which was set to 8 for the analysis), and scaling tests revealed an excellent parallel efficiency of 93.2%.

Molecular dynamics of drug-protein complexes using the supercomputer Expanse

Dynamics were performed in a similar manner to that described by Tang and co-authors.[24] The structures and input files were prepared with the Visual Molecular Dynamics (VMD) package[25] v. 1.9.4 and CHARMM-GUI Ligand Reader and Modeler, which is available on charmm-gui.org. Nanoscale Molecular Dynamics (NAMD) software[26] v. 2.14, running on the SDSC Expanse cluster, was used to simulate 100 ns of Molecular Dynamics (MD), and VMD was used to extract data from the NAMD trajectory files.

Results

Pharmacophore-based docking results

Analysis of the interface of subunit S1 with ACE2 (PDB ID: 6VW1) revealed 29 possible interactions between the two proteins, including 17 residues of ACE2 and 14 residues of the S1 subunit (see Table 1). The binding interface in Figure 1 is clearly split into two interaction sites: Site 1 with ACE2 residues Gln24, Lys26, Thr27, Asp30, Lys31, His34, Glu35, Leu79, Met82, and Tyr83; and Site 2 with ACE2 residues Glu37, Asp38, Tyr41, Gln42, Gly352, Lys353, Gly354, Asp355, and Arg357.

Because our goal is to inhibit binding of the S1 subunit to ACE2, we used the S1 binding domain (Fig. 2) for pharmacophore development. The following residues from both sites were used–Site1: Tyr449, Gly496, Thr500, Asn501, Gly502, and Tyr505; and Site 2: Tyr453, Leu455, Phe456, Tyr473, Phe486, Asn487, Tyr489, and Gln493.

The pharmacophore developed using MOE is based on both interaction sites and consists of 16 centers: 5 acceptors, 4 donors, 2 donor or/and acceptor, and 5 hydrophobics. The pharmacophore search was conducted using an FDA-approved drug database with 2,356 drugs using full and partial pharmacophores. The search with the partial pharmacophore having 6 of 16 features resulted in 379 compounds with 806,486 conformations. After analysis of the binding properties, 152 compounds were selected.

Then, we clustered the selected 152 compounds as described in the *Methods* section. We identified four clusters (A, B, C, and D) in our pharmacophore search of the FDA-approved drug database containing more than ten compounds (18, 18, 14, and 11 correspondingly); three clusters (E, F, and G) containing eight, six, and five compounds correspondingly; three clusters (H, I, and J) with four compounds; three clusters (K, L, and M) with three compounds; and eight two-compound clusters (N-R and T-V) and 35

Table 1. Residues of interface between S1 subunit of S protein and ACE2 receptor

S1 subunit		ACE2		Distance, Å
Residue	Atom	Residue	Atom	
Tyr449	OH [O]	Asp38	OD1 [O]	2.99
Tyr449	OH [O]	Gln42	NE2 [N]	3.73
Tyr453	OH [O]	His34	NE2 [N]	3.84
Leu455	CD2 [C]	Lys31	CD [C]	4.88
Leu455	CD2 [C]	His34	CE1 [C]	4.28
Phe456	CZ [C]	Asp30	CB [C]	4.37
Phe456	CE2 [C]	Lys31	CD [C]	4.12
Tyr473	CE1 {C]	Thr27	CG2 [C]	4.91
Phe486	CD1 [C]	Leu79	CD2 [C]	3.54
Phe486	CD1 [C]	Met82	CE [C]	3.48
Phe486	CE1 {C]	Tyr83	CE2 [C]	3.88
Asn487	ND2 [N]	Gln24	OE1 [O]	3.03
Asn487	OD1 [O]	Tyr83	OH [O]	2.93
Tyr489	CD1 [C]	Lys31	CG [C]	4.02
Gln493	OE1 [O]	Lys31	NZ [N+]	2.92
Gln493	CD [C]	His34	CB [C]	4.55
Gln493	NE2 [N]	Glu35	OE2 [O−]	2.93
Gly496	O [O]	Lys353	NZ [N+]	2.98
Thr500	OG1 [O]	Tyr41	OH [O]	2.62
Thr500	O [O]	Asp355	OD2 [O−]	3.59
Thr500	OG1 [O]	Arg357	NH1 [N]	3.91
Thr500	CB [C]	Arg357	CZ [C]	4.71
Asn501	ND2 [N]	Tyr41	OH [O]	3.29
Asn501	CG [C]	Lys353	CD [C]	4.22
Gly502	N [N]	Lys353	O [O}	2.82
Gly502	N [N]	Gly354	O [O}	3.70
Tyr505	CD1 [C]	Lys353	C [C]	3.31
Tyr505	CD1 [C]	Gly354	CA [C]	4.30
Tyr505	OH [O]	Glu374	OE1 [O]	3.18

Table 2. Drug-candidates clustered by fingerprint similarity–overlap alignment

Cluster						
A	*B*	*C*	*D*	*E*	*F*	*G*
Angiotensin II	Acarbose	Calcifediol[a]	Cefmenoxime	Daunorubicin	Abemaciclib	Alatrofloxacin[a]
Anidulafungin[b]	Amikacin	Calcitriol	Cefonicid	Diosmin	Afatinib	Daclatasvir[b]
Bleomycin	Deslanoside[a]	DMPC*[a]	Cefoperazone	Doxorubicin	Brigatinib	Ombitasvir[b]
Carfilzomib	Dibekacin[a]	Epoprostenol[a]	Ceforanide	Epirubicin	Gilteritinib	Pibrentasvir[a]
Caspofungin	Framycetin[a]	Fingolimod	Cefotetan[a]	FAD**	Imatinib	Pralatrexate
Desmopressin	Gentamicin	Ibutilide	Cefotiam[b]	Hesperidin	Nilotinib	
Etelcalcetide[a]	Hyaluronan[a]	Linoleic acid	Cefpiramide	Mithramycin[a]		
Goserelin	Kanamycin	Lutein	Ceftibuten	Rutin	*H*	*I*
Lanreotide[a]	Lactulose	Montelukast	Ceftobiprole[a]		Flavin mononucleotide[a]	Betaxolol
Lopinavir	Micronomicin[a]	Paricalcitol[a]	Ceftolozane[a]		Regadenoson	Bisoprolol
Nafarelin	Netilmicin	Pravastatin	Latamoxef		Riboflavin	Esmolol
Pentagastrin[a]	Paromomycin	Retapamulin			Ticagrelor	Levobetaxolol
Rifapentine	Pentosan polysulfate[a]	Thonzonium[a]				
Ritonavir	Plazomicin[a]	Vitamin E succinate	*J*	*K*	*L*	*M*
Saquinavir[a]	Ribostamycin		Lymecycline[a]	Ledipasvir	Arformoterol	Dapagliflozin
Tacrolimus	Steviolbioside	*N*	Methacycline	Lusutrombopag[a]	Indacaterol	Empagliflozin
Viomycin[a]	Streptomycin	Glimepiride	Rolitetracycline[a]	Velpatasvir	Protokylol[a]	Ertugliflozin
Xifaxan[a]	Tobramycin	Glyburide	Tigecycline			
O	*P*	*Q*	*R*	*T*	*U*	*V*
Doripenem	Valacyclovir[a]	Irinotecan	Reserpinine[a]	Mitoxantrone	Bosutinib	Florbetaben (18F)[a]
Ertapenem	Valganciclovir	Simeprevir	Vilazodone	Pixantrone	Neratinib	Florbetapir (18F)[a]

*DMPC: Dimyristoylphosphatidylcholine, **FAD: Flavin adenine dinucleotide. [a]Compounds were not tested by Tsegay and colleagues.[27] [b]Compounds have experimentally confirmed activities vs Spike protein.[27]

not clustered single compounds (S). Compounds in clusters A-R and T-V are listed in Table 2, and the 35 single-cluster compounds are provided in Table 3.[27]

To validate the search results and select the best binding drugs, we docked the conformers from the set of 152 drugs selected from the pharmacophore-based search and from a set of 100 random compounds to the binding site of the ACE2 receptor (Protein Data Bank entry, 6VW1).

Multiple conformations molecular docking with Comet results

For more accurate docking, Conformational Import (a special conformer-generating application) was performed on the selected compounds from MOE, resulting in 13,126 conformations. Similarly, MOE Conformational Import was conducted for the 100 random compounds selected from the public ZINC database, resulting in 15,596 conformations.

The 28,722 total conformations were fed into Autodock Vina to find docking poses; 9 docking poses were found per conformation creating a total of 258,498 docking poses. The local SSD and job bundling approach used for Autodock Vina docking runs is described in the *Docking Workflow* subsection in the *Methods* section. The interaction energies of the selected drugs with each of interaction sites of ACE2 are shown in Table 4. Thirteen compounds with highest affinities to both sites listed in Table 5.

The Venn diagram created with Venny server[28] shows that 27 of the top 39 compounds dock to both interaction sites (Fig. 3).

After analyzing the list of common compounds, one can see that ten best compounds with a docking energy less than −7.0 kcal/mol are bound to both sites with higher affinity, half of which belong to cluster A.

The summary of binding energies are shown in Table 6, which includes minimal (*min*), maximal (*max*), median (*med*), and mean (*mean*) values as well as lower *q1* and upper *q3* quartiles. Table 6 also indicates that all binding energies values are better for selected drugs for both sites. The values for both sites are almost identical. Figure 4 illustrates the box plots of docking free energies for the selected drugs and random compounds, which correspond to the first five values of Table 6. In the plots, whiskers represent the minimal and maximal values (q0 and q4), the box outlines the lower and upper quartiles (q1 and q3), and the line with × inside indicates the median (q2). Outliers are plotted as individual points. It is clear from Table 6 and Figure 4 that

Table 3. Compounds that are single in a cluster

Singles (S)					
Novobiocin	Hydrocortamate[a]	Dasatinib[b]	Ponatinib	Bisoctrizole[a]	DPTA*[a]
Calcein[a]	Chlorohexidine	Oxiglutatione[a]	Aliskiren	Curcumin	Betrixaban
Pantethine	Mezlocillin	Panobinostat	Edoxaban[b]	Naldemedine[a]	Siponimod
Bemotrizinol[a]	Cromoglicic acid	Peramivir[a]	Lenvatinib[b]	Tezacaftor	Pegvaliase[a]
Indinavir	Balsalazide	Dabigatran etexilate	Nintedanib	Glasdegib	Netarsudil[a]
Cerivastatin[a]	Ketoconazole	Raltegravir	Sonidegib	Sultamicillin	

*DPTA: Diaminopropanol tetraacetic acid. [a]Compounds were not tested by Tsegay and colleagues.[27] [b]Compounds have experimentally confirmed activities vs Spike protein.[27]

Table 4. Top 40 docked compounds sorted by their energies of interaction with S1 subunit of COVID-19 Spike protein binding sites on ACE2 receptor

SITE1 docking	DFE*	Cluster	SITE2 docking	DFE*	Cluster
Abemaciclib	−9.9	F	Ledipasvir	−9.1	K
Flavin adenine dinucleotide	−9.9	E	Raltegravir	−9.1	S
Nilotinib[b]	−9.9	F	Angiotensin II	−9.0	A
Ponatinib	−9.9	S	Ertapenem	−8.8	O
Saquinavir[a]	−9.9	A	Flavin adenine dinucleotide	−8.6	E
Siponimod	−9.9	S	Velpatasvir[b]	−8.4	K
Vilazodone[b]	−9.9	R	Deslanoside[a]	−8.3	B
Alatrofloxacin	−9.8	G	Arformoterol	−8.1	L
Diosmin	−9.8	E	Indacaterol	−8.1	L
Irinotecan	−9.8	Q	Pibrentasvir[a]	−8.1	G
Naldemedine[a]	−9.8	S	Sonidegib	−8.1	S
Sonidegib	−9.8	S	Siponimod	−8.0	S
Sultamicillin	−9.8	S	Desmopressin	−7.9	A
Glyburide	−9.6	N	Irinotecan	−7.9	Q
Deslanoside[a]	−9.5	B	Afatinib	−7.8	F
Hesperidin	−9.5	E	Diosmin	−7.8	E
Brigatinib	−9.4	F	Lanreotide[a]	−7.8	A
Chlorohexidine	−9.4	S	Mithramycin[a]	−7.8	E
Cromoglicic acid	−9.4	S	Rifapentine	−7.8	A
Novobiocin	−9.4	S	Vilazodone[b]	−7.8	R

[a]Compounds were not tested by Tsegay and colleagues.[27] [b]Compounds have experimentally confirmed activities vs Spike protein.[27]

Table 5. Top 13 docked compounds with highest affinities of interaction energies of COVID-19 Spike protein–ACE2 receptor ranked by average DFE* for both binding Sites 1 and 2

Thirteen top best compounds	Site 1 DFE*	Site 2 DFE*	Cluster
Flavin adenine dinucleotide	−9.9	−8.6	E
Siponimod	−9.9	−8.6	S
Sonidegib	−9.8	−8.1	S
Deslanoside	−9.5	−8.3	B
Irinotecan	−9.8	−7.9	Q
Raltegravir	−8.6	−9.1	S
Vilazodeneb	−9.9	−7.8	R
Ertapenem	−8.9	−8.8	O
Diosmin	−9.8	−7.8	E
Ponatinib	−9.9	−7.6	S
Nilotinib	−9.9	−7.5	F
Alatrofloxacin	−9.8	−7.5	G
Ledipasvir	−8.0	−9.1	K

*Docking free energy, kcal/mol.

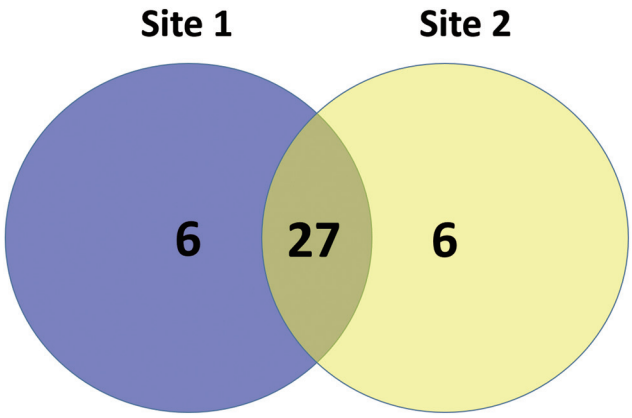

Fig. 3. Venn diagrams of 39 top compounds docked to ACE2 protein. ACE2, angiotensin-converting enzyme 2.

free binding energies are better for selected drugs than random compounds.

Note that the values of docking energy were only used to prioritize compounds for further experimental testing. In general, all of the pharmacophore-selected drugs could be valuable inhibitors.

Molecular dynamics results

Given the results from Autodock Vina, the top five drugs with the best binding energies were selected for validation with MD. Figure 5 shows the positions of the top binding drugs after 100-ns MD, which are within the initial binding sites of these drugs. Figure 6 displays the simulations results by tracking the distance between the geometric centers of each drug and an arbitrary residue in each binding site over time. The plots indicate the stability of the drug complexes with ACE2, in which most drugs have distances that remain mostly stable.

Discussion

Based on the crystal structure of the SARS-CoV-2 chimeric receptor binding domain (PDB ID: 6VW1),[19] we created a pharmacophore model of the interface of this protein and ACE2 to screen a conformational database of FDA-approved drugs. Of the 379 identified drugs, 152 were selected and clusterized to determine the most promising candidates. Then, the selected drugs were used for multi-conformational docking to the interface region of ACE2. The drug list selected includes drugs tested for the treatment of viral infections. In particular, the following drugs that were found using the DrugVirus.info database[29] have been reported in various studies for the treatment of several viruses (Fig. 7).

We created a conformational set of 100 random compounds from the ZINC database and performed multi-conformational docking of these compounds to the interface region of ACE2. After comparing these results with the docking results for the selected drugs, the range of significance in the values of binding energies was found to be moderately better for the selected drugs than the randomly selected drugs. Note that the pharmacophore-based search of the conformational databases by itself identified possible valuable therapeutic compounds, and the calculated docking energies may be useful for prioritizing these candidates for further investigation.

We further note that eight of the drugs selected by the pharmacophore-based database screening have already been tested in various experimental and clinical settings.

In cluster A (Table 2), ritonavir and lopinavir were shown to be effective in treatment of COVID-19 patients. Compared to treatment with pneumonia-associated adjuvant drugs alone, the combination therapy of lopinavir/ritonavir and adjuvant drugs has a more evident therapeutic effect in restoring normal health of the patients with no toxic side effects.[30] Saquinavir demonstrated antiviral activity, as quantified by Taqman RT-PCR. Drug-induced effects on cells were monitored by quantifying LDH release and ATP levels.[31]

In cluster C (Table 2), three drugs have been tested by others scientists. In an ELISA assay, calcitriol was found to inhibit the receptor binding domain of SARS-CoV-2 S1 interaction with ACE2 at both low and high concentrations.[32] Khan and colleagues reported montelukast to be associated with a reduction in clinical deterioration for COVID-19 confirmed patients.[33] Jonsson and coauthors demonstrated that the duration of COVID-19 symptoms can be shortened by early initiation of nebulized isomerized linoleic acid in outpatient treatment.[34] A recent pilot study indicates that calcitriol may decrease hospitalization and increase oxygenation.[35]

In cluster E (Table 2), the molecule similar to rutin–quercetin–was tested by Pan and colleagies.[36] Interaction of quercetin with ACE2 was confirmed by a surface plasmon resonance assay, which showed that rutin (quercetin) interacts strongly with the main protease $3CL^{pro}$.[36]

In cluster G (Table 2), daclatasvir showed to prolong the life expectancy of COVID-19 patients.[37]

Our approach uses a well-understood methodology to identify a set of existing, approved drugs that have therapeutic potential in treating individuals infected with SARS-CoV-2. The methodology identified a group of drugs that have been shown to improve the treatment outcomes of SARS-CoV-2 and related viral infections, compounds that are currently under active investigation, as well as a group of related drugs that have not yet been investigated. The calculated binding energies for the related drugs provide a basis on

Table 6. Summary of binding energies (kcal/mol) for selected drugs and random FDA-approved compounds

	min	q1	med	q3	max	mean
SITE 1						
Selected	−9.9	−8.7	−8.2	−7.5	−5.9	−8.16
Random	−9.8	−8.1	−7.4	−6.4	−3.4	−7.17
SITE 2						
Selected	−9.1	−7.4	−6.80	−6.4	−4.9	−6.89
Random	−8.7	−7.0	−6.4	−5.5	−3.4	−6.29

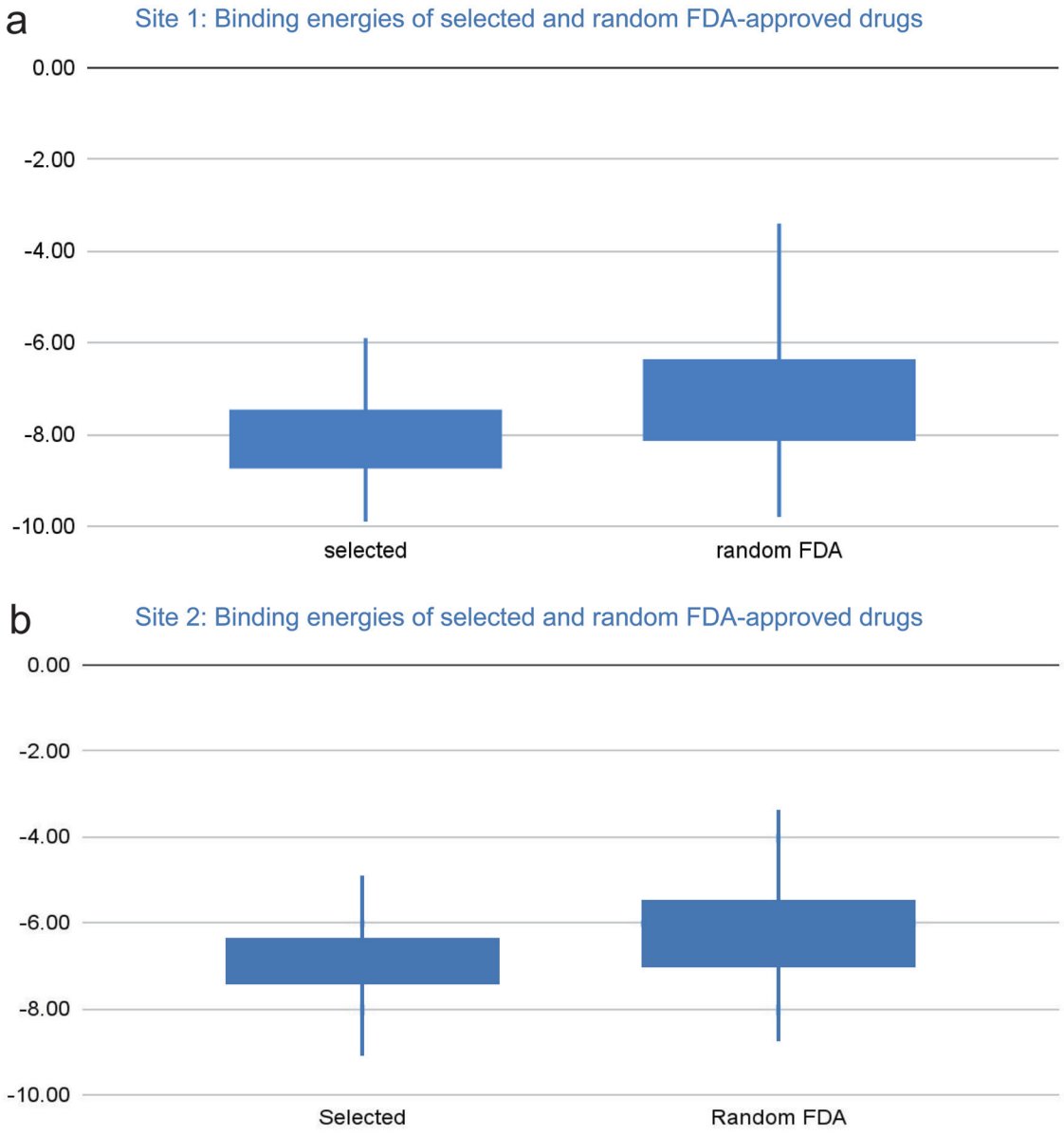

Fig. 4. Free energies of docking interactions of selected and random FDA-approved compounds with both binding sites of ACE2. Minimal energies of the selected and random compounds for are (a) −9.9 and −9.8 kcal/mol for Site 1 and (b) −9.1 and −8.7 kcal/mol for Site 2, respectively. ACE2, angiotensin-converting enzyme 2.

which to prioritize further experimental and clinical investigations on the potential impact of these compounds in treating COVID-19.

Relation to experimental results

Recently, Tsegay and colleagues reported the results of binding experiments with a similar set of pre-approved pharmaceutical compounds.[27] This work provides an opportunity to evaluate the screening method reported in our presented work.

True Positives: Of the 39 compounds examined in our final screen, 3 drugs, namely nilotinib, velpatasvir, and vilazodone, were found to significantly inhibit Spike protein binding, with EC_{50} values of 4.2, 15, and 70 μM, respectively.[27] Binding inhibition by the tyrosine kinase inhibitor nilotinib was also confirmed by Chtita and colleagues,[38] owing to its strong binding to the ACE protease. Recent reports show that nilotinib inhibits viral replication in cell culture, with a low EC_{50} of 1.88 μM,[39] and exhibits potential as a therapeutic agent. On the other hand, initial clinical trials indicate that vilazodone is ineffective for the treatment of COVID-19 in humans.[40]

False Positives: Of the top 39 candidates identified through our second screen, 26 were also examined by Tsegay and co-authors.[27] Of the total 46 drugs that significantly inhibit ACE protease/Spike protein binding in vitro ($EC_{50} < 10^{-4}$ M), only the three noted above (nilotinib, velpatasvir, and vilazodone) showed significant inhibition of Spike protein binding to the ACE2 protease. Further experiments are needed to evaluate the status of the remaining seven candidates.

False negatives: Of the 152 compounds that showed promise

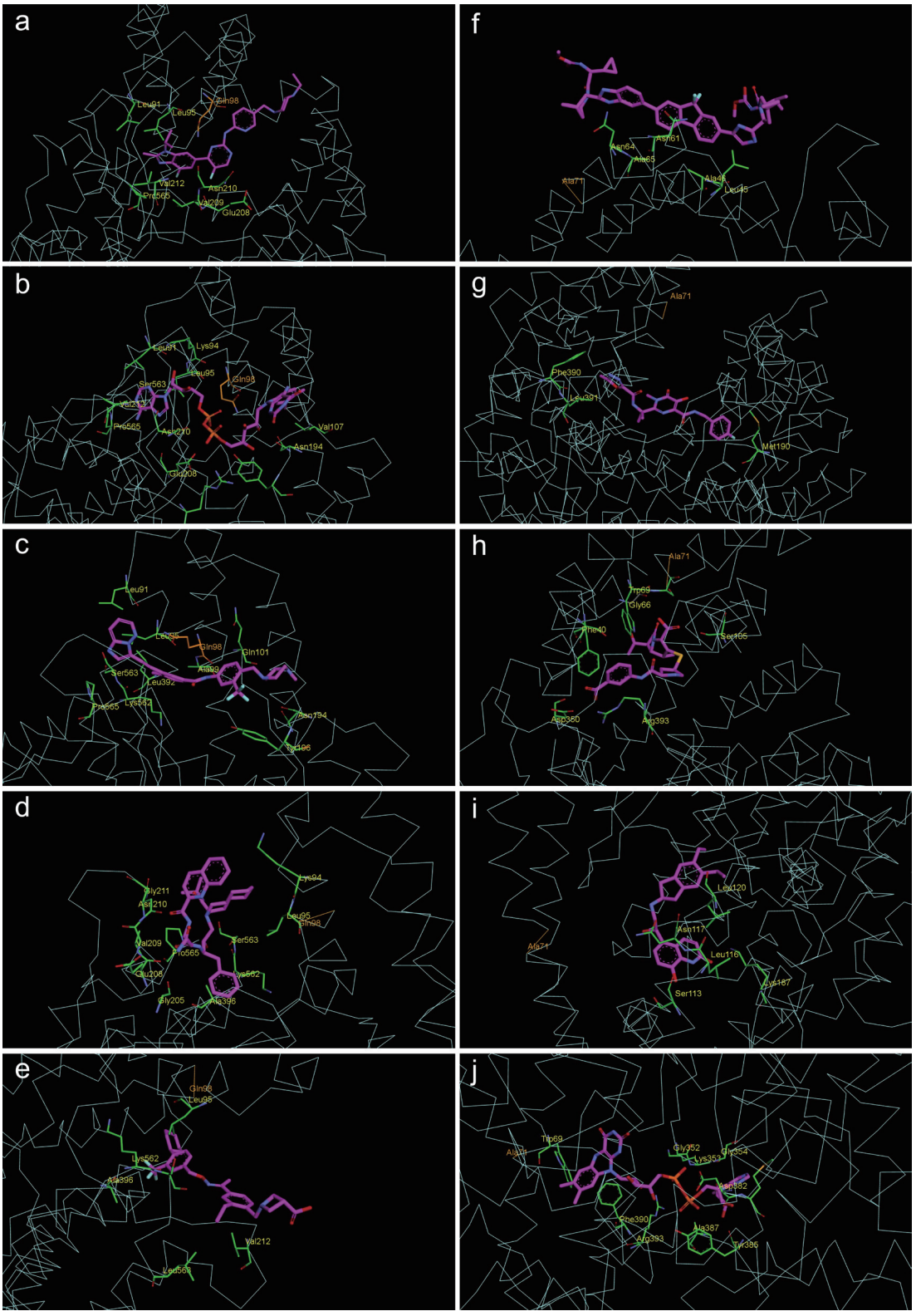

Fig. 5. Binding positions of the drugs with the best scores in ACE2 receptor after 100-ns MD and their docking free energy (DFE) in (a–e) Site 1 and (f–h) Site 2: (a) Abemaciclib, –9.9 kcal/mol. (b) Flavin adenine dinucleotide (FAD), –9.9 kcal/mol. (c) Ponatinib, –9.9 kcal/mol. (d) Saquinavir, –9.9 kcal/mol. (e) Siponimod, –9.9 kcal/mol. (f) Ledipasvir, –9.1 kcal/mol. (g) Raltegravir, –9.1 kcal/mol. (h) Ertapenem, –8.8 kcal/mol. (i) Indacaterol, –8.1 kcal/mol. (j) FAD, –8.6 kcal/mol. ACE2, angiotensin-converting enzyme 2; DFE, docking free energy; MD, molecular dynamics.

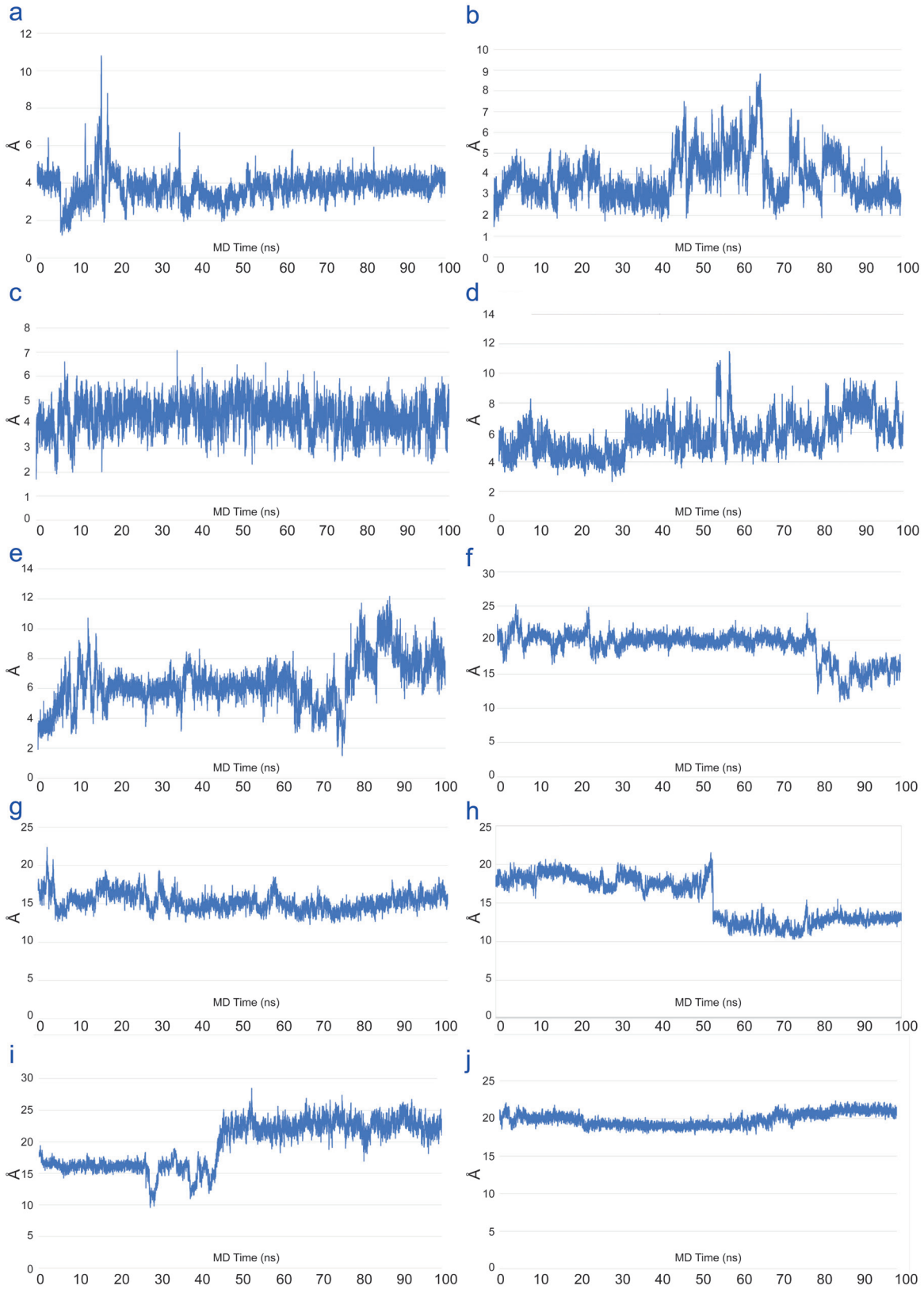

Fig. 6. Plots of distances between the center coordinates of the docked compounds and a common residue in the binding site after 100 ns of MD, showing that the complexes are relatively stable. Plots a–h correspond to the compounds in Figure 5. MD, molecular dynamics.

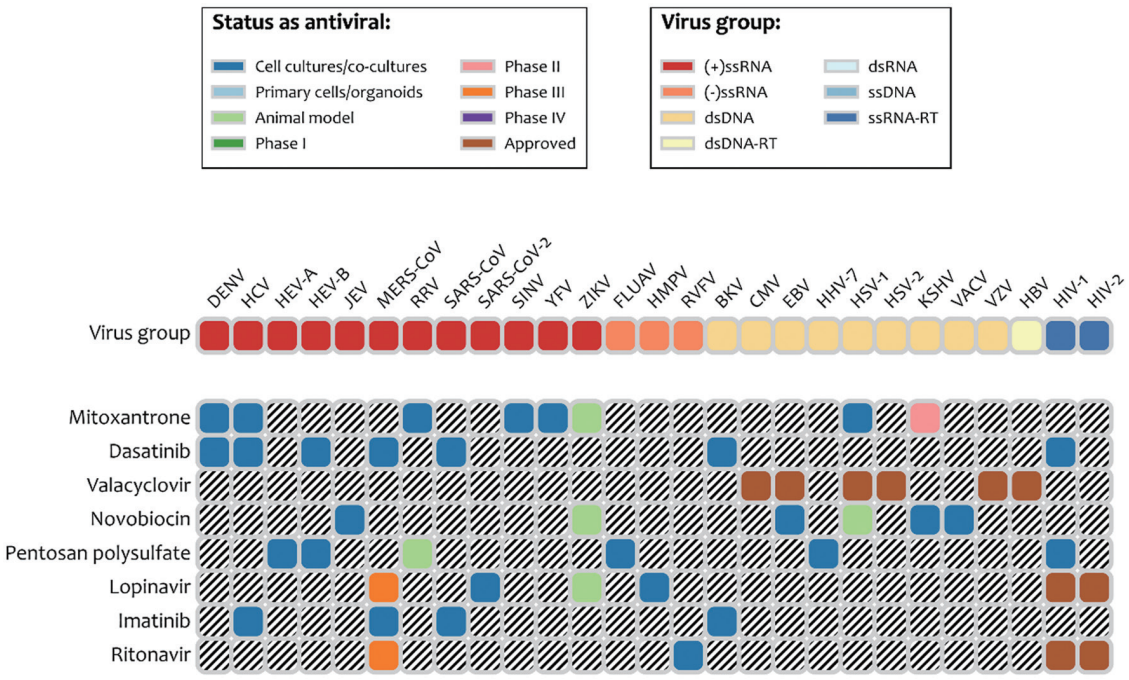

Fig. 7. Selected drugs that have been experimentally tested for various viruses (data obtained using DrugVirus.info database[29]). These drugs include: *Valacyclovir,* (Group P) is approved for treatment of the following viral infections: CMV, EBV, HSV-1, HSV-2, VZV, and HBV; *Lopinavir,* (Group A) is approved for treatment of HIV-1 and HIV-2; in phase III trials for treatment of MERS-CoV; in animal studies for treatment of ZIKV; and in cell-culture studies for treatment of HMPV and SARS-CoV-2; *Ritonavir*, (Group A) is approved for treatment of HIV-1 and HIV-2; in phase III trials for treatment of MERS-CoV; in animal studies for treatment of ZIKV; and in cell-culture studies for treatment of RVFV; *Mitoxantrone*, (Group T) is in phase II trials for treatment of KSHV; in animal models for treatment of ZIKV; and in cell-cultures for treatment of DENV, HCV, RRV, SINV, YFV, and HSV-1; *Novobiocin*, (Single) is being studied in animal models for treatment of ZIKV and HSV-1 and in cell-cultures for treatment of JEV, EBV, KHSV, and VACV; *Pentosan polysulphate* (Group B) is being studied in animal models for treatment of RRV and in cell-cultures for treatment of HEV-A, HEV-B, HMPV, and HHV-7; *Imatinib*, (Group F) is being studied in cell-cultures for treatment of, HCV, MERS-CoV, SARS-CoV, and BKV.

in our initial virtual screen, 7 exhibited inhibition of Spike protein binding in vitro (EC_{50} < 75 μM),[27] which include: anidulafungin; cefotiam hexetil hydrochloride; daclatasvir, ombitasvir; dasatinib; edoxaban; and lenvatinib mesylate. However, these compounds were not among the top 39 in our secondary docking screening, indicating that the pharmacophore search alone is an effective tool for selection of potential drug candidates. The results presented here provide an opportunity to further tune our screening protocol.

Future directions

After further experimental testing of the suggested compounds for repurposing drugs, we plan to improve the pharmacophore model based on the residues and molecules that participate in the binding of compounds to both sides of ACE2. Subsequently, molecular docking would be conducted.

Conclusions

A set of FDA-approved drug compounds with the best parameters for interacting with the spike protein of SARS-CoV-2 is presented. The compounds were identified considering consistently several steps. Pharmacophore was developed on the basis of the ACE2 residues that participate in the interface with the SARS-CoV-2 spike protein. Pharmacophore-based docking, and unrestrained molecular docking of the compounds to the ACE2 were conducted. The stability of the selected compounds' binding to ACE2 was confirmed by 100-ns molecular-dynamics simulation of the bound protein–drug complexes. We suggest that the selected drugs might bind to the interface of the ACE2/spike protein of SARS-CoV-2 and prevent spike binding to ACE2. We suggest further testing of the selected compounds for treatment of COVID-19 in future works.

Acknowledgments

We would like to thank the people of the San Diego Supercomputer Center for their friendly support.

Funding

The SDSC Comet supercomputer is supported by the NSF grant: ACI #1341698 Gateways to Discovery: Cyberinfrastructure for the Long Tail of Science. The SDSC Expanse Cluster by the NSF grant: #1928224 Computing without Boundaries: Cyberinfrastructure for the Long Tail of Science.

Conflict of interest

Prof. Igor F. Tsigelny has been an associate editor of *Journal of*

Exploratory Research in Pharmacology since November 2021. Prof. Igor F. Tsigelny is a President of BiAna, and Prof. Valentina L. Kouznetsova is the CEO of BiAna. The authors have no other conflicts of interest related to this publication.

Author contributions

IFT and VLK introduced the basic idea of the project. VLK conducted pharmacophore models development, databases searches, pharmacophore-based clustering and multiconformational alignment. MAM, IFT, and VLK conducted interpretation of the results. AZ and MT conducted computational docking on the Comet supercomputer. JPG conducted molecular dynamics simulations on Expanse cluster. IFT, VLK, MAM, and AZ wrote the article. VLK, MAM, and AZ contributed equally to this work.

Data sharing statement

No additional data are available.

References

[1] Zhou Y, Vedantham P, Lu K, Agudelo J, Carrion R Jr, Nunneley JW, *et al*. Protease inhibitors targeting coronavirus and filovirus entry. Antivir Res 2015;116:76–84. doi:10.1016/j.antiviral.2015.01.011.

[2] Huang Y, Yang C, Xu XF, Xu W, Liu SW. Structural and functional properties of SARS-CoV-2 spike protein: potential antivirus drug development for COVID-19. Acta Pharmacol Sin 2020;41(9):1141–1149. doi:10.1038/s41401-020-0485-4.

[3] Hoffmann M, Kleine-Weber H, Schroeder S, Krüger N, Herrler T, Erichsen S, *et al*. SARS-CoV-2 Cell Entry Depends on ACE2 and TMPRSS2 and Is Blocked by a Clinically Proven Protease Inhibitor. Cell 2020;181(2):271–280.e8. doi:10.1016/j.cell.2020.02.052.

[4] Li F, Li W, Farzan M, Harrison SC. Structure of SARS coronavirus spike receptor-binding domain complexed with receptor. Science 2005; 309(5742):1864–1868. doi:10.1126/science.1116480.

[5] Zhou P, Yang XL, Wang XG, Hu B, Zhang L, Zhang W, *et al*. A pneumonia outbreak associated with a new coronavirus of probable bat origin. Nature 2020;579(7798):270–273. doi:10.1038/s41586-020-2012-7.

[6] Lan J, Ge J, Yu J, Shan S, Zhou H, Fan S, *et al*. Structure of the SARS-CoV-2 spike receptor-binding domain bound to the ACE2 receptor. Nature 2020;581(7807):215–220. doi:10.1038/s41586-020-2180-5.

[7] Li W, Zhang C, Sui J, Kuhn JH, Moore MJ, Luo S, *et al*. Receptor and viral determinants of SARS-coronavirus adaptation to human ACE2. EMBO J 2005;24(8):1634–1643. doi:10.1038/sj.emboj.7600640.

[8] Walls AC, Park YJ, Tortorici MA, Wall A, McGuire AT, Veesler D. Structure, Function, and Antigenicity of the SARS-CoV-2 Spike Glycoprotein. Cell 2020;181(2):281–292.e6. doi:10.1016/j.cell.2020.02.058.

[9] Glowacka I, Bertram S, Müller MA, Allen P, Soilleux E, Pfefferle S, *et al*. Evidence that TMPRSS2 activates the severe acute respiratory syndrome coronavirus spike protein for membrane fusion and reduces viral control by the humoral immune response. J Virol 2011;85(9):4122–4134. doi:10.1128/JVI.02232-10.

[10] Matsuyama S, Nagata N, Shirato K, Kawase M, Takeda M, Taguchi F. Efficient activation of the severe acute respiratory syndrome coronavirus spike protein by the transmembrane protease TMPRSS2. J Virol 2010;84(24):12658–12664. doi:10.1128/JVI.01542-10.

[11] Shulla A, Heald-Sargent T, Subramanya G, Zhao J, Perlman S, Gallagher T. A transmembrane serine protease is linked to the severe acute respiratory syndrome coronavirus receptor and activates virus entry. J Virol 2011;85(2):873–882. doi:10.1128/JVI.02062-10.

[12] Zhao X, Guo F, Comunale MA, Mehta A, Sehgal M, Jain P, *et al*. Inhibition of endoplasmic reticulum-resident glucosidases impairs severe acute respiratory syndrome coronavirus and human coronavirus NL63 spike protein-mediated entry by altering the glycan processing of angiotensin I-converting enzyme 2. Antimicrob Agents Chemother 2015;59(1):206–216. doi:10.1128/AAC.03999-14.

[13] Tian X, Li C, Huang A, Xia S, Lu S, Shi Z, *et al*. Potent binding of 2019 novel coronavirus spike protein by a SARS coronavirus-specific human monoclonal antibody. Emerg Microbes Infect 2020;9(1):382–385. doi:10.1080/22221751.2020.1729069.

[14] Wrapp D, Wang N, Corbett KS, Goldsmith JA, Hsieh C-L, Abiona O, *et al*. Cryo-EM structure of the 2019-nCoV spike in the prefusion conformation. Science 2020;367(6483):1260–1263. doi:10.1126/science.abb2507.

[15] Pinto D, Park Y-J, Beltramello M, Walls AC, Tortorici MA, Bianchi S, *et al*. Cross-neutralization of SARS-CoV-2 by a human monoclonal SARS-CoV antibody. Nature 2020;583(7815):290–295. doi:10.1038/s41586-020-2349-y.

[16] Shi R, Shan C, Duan X, Chen Z, Liu P, Song J, *et al*. A human neutralizing antibody targets the receptor binding site of SARS-CoV-2. Nature 2020;584(7819):120–124. doi:10.1038/s41586-020-2381-y.

[17] Baum A, Fulton BO, Wloga E, Copin R, Pascal KE, Russo V, *et al*. Antibody cocktail to SARS-CoV-2 spike protein prevents rapid mutational escape seen with individual antibodies. Science 2020;369(6506):1014–1018. doi:10.1126/science.abd0831.

[18] Li W, Moore MJ, Vasilieva N, Sui J, Wong SK, Berne MA, *et al*. Angiotensin-converting enzyme 2 is a functional receptor for the SARS coronavirus. Nature 2003;426(6965):450–454. doi:10.1038/nature02145.

[19] Shang J, Ye G, Shi K, Wan Y, Luo C, Aihara H, *et al*. Structural basis of receptor recognition by SARS-CoV-2. Nature 2020;581(7807):221–224. doi:10.1038/s41586-020-2179-y.

[20] MOE: Molecular Operating Environment. Montreal: Chemical Computing Group ULC; 2019. Available from: https://www.chemcomp.com/. Accessed September 20, 2021.

[21] Trott O, Olson AJ. AutoDock Vina: Improving the speed and accuracy of docking with a new scoring function, efficient optimization, and multithreading. J Comput Chem 2010;31(2):455–461. doi:10.1002/jcc.21334.

[22] Strande SM, Cai H, Cooper T, Flammer K, Irving C, von Laszewski G, *et al*. Comet: Tales from the Long Tail: Two Years In and 10,000 Users Later. In: Proceedings of the Practice and Experience in Advanced Research Computing 2017 on Sustainability, Success and Impact. New York, NY, USA: Association for Computing Machinery; 2017:1–7. doi:10.1145/3093338.3093383.

[23] Kouznetsova VL, Zhang A, Tatineni M, Miller MA, Tsigelny IF. Potential COVID-19 papain-like protease PL^{pro} inhibitors: repurposing FDA-approved drugs. PeerJ 2020;8:e9965. doi:10.7717/peerj.9965.

[24] Tang JY, Tsigelny IF, Greenberg JP, Miller MA, Kouznetsova VL. Potential SARS-CoV-2 nonstructural protein 15 inhibitors: repurposing FDA-approved drugs. J Explor Res Pharmacol 2021;6(4):137–147. doi:10.14218/JERP.2021.00032.

[25] Eargle J, Wright D, Luthey-Schulten Z. Multiple Alignment of protein structures and sequences for VMD. Bioinformatics 2006;22(4):504–506. doi:10.1093/bioinformatics/bti825.

[26] Phillips JC, Hardy DJ, Maia JDC, Stone ES, Ribeiro JV, Bernardi RC, *et al*. Scalable molecular dynamics on CPU and GPU architectures with NAMD. J Chem Phys 2020;153(4):044130. doi:10.1063/5.0014475.

[27] Tsegay KB, Adeyemi CM, Gniffke EP, Sather DN, Walker JK, Smith SEP. A repurposed drug screen identifies compounds that inhibit the binding of the COVID-19 spike protein to ACE2. Front Pharmacol 2021;12:685308. doi:10.3389/fphar.2021.685308.

[28] Oliveros JC. Venny: An interactive tool for comparing lists with Venn's diagrams. 2007-2015. Available from: https://bioinfogp.cnb.csic.es/tools/venny/index.html. Accessed September 23, 2021.

[29] Andersen PI, Ianevski A, Lysvand H, Vitkauskiene A, Oksenych V, Bjørås M, *et al*. Discovery and development of safe-in-man broad-spectrum antiviral agents. Int J Infect Dis 2020;93:268–276. doi:10.1016/j.ijid.2020.02.018.

[30] Ye XT, Luo YL, Xia SC, Sun QF, Ding JG, Zhou Y, *et al*. Clinical efficacy of lopinavir/ritonavir in the treatment of Coronavirus disease 2019. Eur Rev Med Pharmacol Sci 2020;24(6):3390–3396. doi:10.26355/eurrev_202003_20706.

[31] Farag A, Wang P, Boys IN, Eitson JL, Ohlson M, Fan W, *et al*. Identification of atovaquone, ouabain and mebendazole as FDA approved drugs targeting SARS-CoV-2 (Version 4). ChemRxiv 2020. doi:10.26434/

chemrxiv.12003930.v4.

[32] Fu W, Chen Y, Wang K, Hettinghouse A, Hu W, Wang JQ, *et al*. Repurposing FDA-approved drugs for SARSCoV-2 through an ELISA-based screening for the inhibition of RBD/ACE2 interaction. Protein Cell 2021;12(7):586–591. doi:10.1007/s13238-020-00803-w.

[33] Khan A, Misdary C, Yegya-Raman N, Kim S, Narayanan N, Siddiqui S, *et al*. Montelukast in hospitalized patients diagnosed with COVID-19. J Asthma 2021:1–7. doi:10.1080/02770903.2021.1881967.

[34] Jonsson S, Mendenhall M, Jonsson C. Case study using nebulized isomerized linoleic acid (LA) for outpatient treatment of symptomatic COVID-19. SSRN 2020;doi:10.2139/ssrn.3733231.

[35] Elamir Y, Amir H, Feliciano N, Gonzalez C, Grist W, Lim S, *et al*. Abstract #1002919: Endocrine therapy for COVID19: A randomized pilot study using calcitriol. Endocr Pract 2021;27(6):S79. doi:10.1016/j.eprac.2021.04.636.

[36] Pan B, Fang S, Zhang J, Pan Y, Liu H, Wang Y, *et al*. Chinese herbal compounds against SARS-CoV-2: Puerarin and quercetin impair the binding of viral S-protein to ACE2 receptor. Comput Struct Biotechnol J 2020;18:3518–3527. doi:10.1016/j.csbj.2020.11.010.

[37] Eslami G, Mousaviasl S, Radmanesh E, Jelvay S, Bitaraf S, Simmons B, *et al*. The impact of sofosbuvir/daclatasvir or ribavirin in patients with severe COVID-19. J Antimicrob Chemother 2020;75(11):3366–3372. doi:10.1093/jac/dkaa331.

[38] Chtita S, Belhassan A, Aouidate A, Belaidi S, Bouachrine M, Lakhlifi T. Discovery of Potent SARS-CoV-2 Inhibitors from Approved Antiviral Drugs via Docking and Virtual Screening. Comb Chem High Throughput Screen 2021;24(3):441–454. doi:10.2174/1386207323999200730205447.

[39] Cagno V, Magliocco G, Tapparel C, Daali Y. The tyrosine kinase inhibitor nilotinib inhibits SARS-CoV-2 in vitro. Basic Clin Pharmacol Toxicol 2021;128(4):621–624. doi:10.1111/bcpt.13537.

[40] Sayad B, Khodarahmi R, Najafi F, Miladi R, Mohseni Afshar Z, Mansouri F, *et al*. Efficacy and safety of sofosbuvir/velpatasvir versus the standard of care in adults hospitalized with COVID-19: A single-centre, randomized controlled trial. J Antimicrob Chemother 2021;76(8):2158–2167. doi:10.1093/jac/dkab152.